ELSEVIER

Lithos 62 (2002) 1–13

LITHOS

www.elsevier.com/locate/lithos

Empirical garnet–muscovite geothermometry in metapelites

Chun-Ming Wu [a,*], Xin-She Wang [b], Chong-Hui Yang [b], Yuan-Sheng Geng [b], Fu-Lai Liu [b]

[a] *Department of Earth Sciences, The Graduate School, Chinese Academy of Sciences, P.O. Box 3908, Beijing 100039, China*
[b] *Institute of Geology, Chinese Academy of Geological Sciences, 26 Baiwanzhuang Street, Beijing 100037, China*

Received 16 August 2001; accepted 18 February 2002

Dedicated to Prof. Qi-Han Shen's 80th birthday

Abstract

Two empirical garnet–muscovite geothermometers, assuming no ferric iron (Model A) and 50% ferric iron (Model B) in muscovite, respectively, were calibrated under the physical conditions of $P = 3.0–14.0$ kbar and $T = 530–700$ °C. The input temperatures and pressures were determined by simultaneously applying the garnet–biotite thermometer [Am. Mineral. 85 (2000) 881.] and the GASP geobarometer [Am. Mineral. 86 (2001) 1117.] to natural metapelites. To confirm internal thermodynamic consistency, Holdaway's [Am. Mineral. 85 (2000) 881.] garnet mixing properties were adopted. Muscovite was treated as a symmetric Fe–Mg–Al^{VI} ternary solid solution, and its Margules parameters were derived in this work. The resulting two formulae reproduced the input garnet–biotite temperatures well within ± 50 °C, and gave identical results for a great body of natural samples. Moreover, they successfully distinguished the systematic changes of temperatures of different grade rocks from a prograde sequence, inverted metamorphic zone, and thermal contact aureole. Pressure estimation has almost no effect on the two formalisms of the garnet–muscovite geothermometer. Assuming analytical error of ± 5% for the relevant components of both garnet and muscovite, the total random uncertainty of the two formulations will generally be within ± 5 °C. The two thermometers derived in this work may be used as practical tools to metamorphic pelites under the conditions of 480 to 700 °C, low- to high-pressure, in the composition ranges Xalm = 0.51–0.82, Xpyr = 0.04–0.22, and Xgros = 0.03–0.24 in garnet, and Fe_{tot} = 0.03–0.17, and Mg = 0.04–0.14 atoms p.f.u. in muscovite.

Keywords: Garnet–muscovite thermometry; Ferric iron; Calibration; Random error

1. Introduction

The partitioning of Fe^{2+} and Mg between coexisting garnet and muscovite, like many other coexisting ferromagnesian mineral pairs, has been calibrated as a geothermometer, either experimentally (Krogh and Raheim, 1978; Green and Hellman, 1982) or empirically (Hynes and Forest, 1988).

However, when these thermometers are applied to natural rocks, large discrepancies between the garnet–muscovite and the garnet–biotite temperatures are not uncommon. Generally, the Krogh and Raheim (1978) and the Hynes and Forest (1988) thermometers underestimate temperatures, whereas the Green and Hellman (1982) thermometer overestimates temperatures. Furthermore, these formulations do not discern the

* Corresponding author. Tel.: +86-10-68229894; fax: +86-10-68226012.
E-mail address: wucm@earth.gscas.ac.cn (C.-M. Wu).

0024-4937/02/$ - see front matter
PII: S0024-4937(02)00096-8

systematic change of temperatures of rocks from different zones of prograde sequences, inverted metamorphic zones, or thermal contact aureoles.

Considering multiphase equilibria, temperatures and pressures computed through different mineral pairs or mineral assemblages should always converge to a unique definite value. Thus, in this paper, we empirically refined the garnet–muscovite thermometry through simultaneously applying the garnet–biotite geothermometer (Holdaway, 2000) and the GASP geobarometer (Holdaway, 2001) to natural metapelitic samples collected from the literature, and we adopted the same composition–activity relations of garnet as Holdaway (2000, 2001). Considering the iron valence, we developed two formulations, for ferric iron-free, and 50% ferric iron contents in muscovite, respectively. We expect that this thermometer may play an important role in determining metamorphic conditions for metapelites, especially when biotite is absent in the rocks, e.g., garnet–muscovite–quartz schists.

2. Thermodynamic basis

The Fe and Mg exchange between coexisting garnet and muscovite can be described as (Krogh and Raheim, 1978; Green and Hellman, 1982; Hynes and Forest, 1988):

$$\underset{\text{pyrope}}{Mg_3Al_2Si_3O_{12}} + 3K(FeAl)Si_4O_{10}(OH)_2 \quad \underset{\text{Fe-celadonite}}{}$$

$$= \underset{\text{almandine}}{Fe_3Al_2Si_3O_{12}} + 3K(MgAl)Si_4O_{10}(OH)_2 \quad \underset{\text{Mg-celadonite}}{} \qquad (1)$$

At equilibrium, the Gibbs free energy change of reaction (1), ΔG, is zero. This leads to the following expression

$$\Delta G = 0 = \Delta H^0 - T\Delta S^0 + (P-1)\Delta V^0 + 3RT\ln K_d + 3RT\ln(\gamma_{Fe}/\gamma_{Mg})^{grt} + 3RT\ln(\gamma_{Mg}/\gamma_{Fe})^{mus} \qquad (2)$$

in which ΔH^0, ΔS^0, and ΔV^0 are the standard enthalpic, entropic, and volumetric changes of reaction (1) at 298.15 K and 1 bar, respectively. K_d is the distribution coefficient, defined as $K_d=(Fe^{2+}/Mg)^{grt}/(Fe^{2+}/Mg)^{mus}$. R is the gas constant, $R=8.3144$ J/mol·K. The last two items in Eq. (2) describe the non-ideal mixing properties of garnet and muscovite, respectively. Thermal expansion and compressibility coefficients of garnet and muscovite were neglected.

2.1. Garnet solid solution

For this study, we adopted the same garnet activity model of Holdaway (2000, 2001), in order to maintain internal thermodynamic consistency between the garnet–biotite and garnet–muscovite thermometers. The Holdaway garnet model is an Fe–Mg–Ca–Mn asymmetric quaternary solid solution, consisting of the Mukhopadhyay et al. (1997) Margules parameters for the asymmetric Fe–Mg–Ca interactions in garnet including a ternary interaction parameter W^{grt}_{FeMgCa}= 7398 J/mol, and symmetric Mn-related parameters $W^{grt}_{MnCa}=W^{grt}_{CaMn}=1425$ J/mol (Ganguly and Cheng, 1994), $W^{grt}_{MnFe}=W^{grt}_{FeMn}=1617$ J/mol (Pownceby et al., 1991), and $W^{grt}_{MnMg}=W^{grt}_{MgMn}=41{,}249-23.01\ T$ J/mol (corrected from Ganguly and Cheng, 1994).

According to Holdaway (2000, 2001), the ratio of activity coefficient of almandine and pyrope in garnet, on the three-ion basis, is

$$3RT\ln(\gamma_{Fe}/\gamma_{Mg})^{grt} = GaT(K) + GbP(bars) + Gc \qquad (3)$$

in which Ga, Gb and Gc are polynomial expressions of garnet components

$$\begin{aligned} Ga = {} & 12.4(X^{grt}_{Fe})^2 + 22.09(X^{grt}_{Mg})^2 - 12.02(X^{grt}_{Ca})^2 \\ & + 23.01(X^{grt}_{Mn})^2 - 68.98(X^{grt}_{Fe})(X^{grt}_{Mg}) \\ & + 37.33(X^{grt}_{Fe})(X^{grt}_{Ca}) + 18.165(X^{grt}_{Fe})(X^{grt}_{Mn}) \\ & + 35.33(X^{grt}_{Mg})(X^{grt}_{Ca}) + 27.855(X^{grt}_{Mg})(X^{grt}_{Mn}) \\ & + 35.165(X^{grt}_{Ca})(X^{grt}_{Mn}) \end{aligned} \qquad (4)$$

$$\begin{aligned} Gb = {} & -0.05(X^{grt}_{Fe})^2 - 0.034(X^{grt}_{Mg})^2 - 0.005(X^{grt}_{Ca})^2 \\ & - 0.014(X^{grt}_{Mn})^2 + 0.168(X^{grt}_{Fe})(X^{grt}_{Mg}) \\ & + 0.1565(X^{grt}_{Fe})(X^{grt}_{Ca}) - 0.022(X^{grt}_{Fe})(X^{grt}_{Mn}) \\ & - 0.2125(X^{grt}_{Mg})(X^{grt}_{Ca}) - 0.006(X^{grt}_{Mg})(X^{grt}_{Mn}) \\ & - 0.0305(X^{grt}_{Ca})(X^{grt}_{Mn}) \end{aligned} \qquad (5)$$

and

$$\begin{aligned}Gc = &-22265.0(X_{Fe}^{grt})^2 - 24166.0(X_{Mg}^{grt})^2 \\ &+ 3220.0(X_{Ca}^{grt})^2 - 39632.0(X_{Mn}^{grt})^2 \\ &+ 92862.0(X_{Fe}^{grt})(X_{Mg}^{grt}) - 67328.0(X_{Fe}^{grt})(X_{Ca}^{grt}) \\ &- 38681.5(X_{Fe}^{grt})(X_{Mn}^{grt}) - 99262.0(X_{Mg}^{grt})(X_{Ca}^{grt}) \\ &- 40582.5(X_{Mg}^{grt})(X_{Mn}^{grt}) - 79669.5(X_{Ca}^{grt})(X_{Mn}^{grt})\end{aligned} \quad (6)$$

respectively.

2.2. Muscovite solid solution

Muscovite was treated as a symmetric Fe–Mg–Al^{VI} ternary solid solution. According to the general formulation for symmetric solutions (Mukhopadhyay et al., 1993), the ration of activity coefficients of Mg- and Fe-celadonite can be written as

$$\begin{aligned}&3RT\ln(\gamma_{Mg}/\gamma_{Fe})^{mus} \\ &\quad = W_{FeMg}^{mus} \cdot 3(X_{Fe}^{mus} - X_{Mg}^{mus}) \\ &\qquad + (W_{MgAl}^{mus} - W_{FeAl}^{mus}) \cdot 3X_{Al}^{mus}\end{aligned} \quad (7)$$

in which the W's are Margules parameters, and the molar fractions of the components are defined as $X_{Fe}^{mus} = Fe^{2+}/(Fe^{2+} + Mg + Al^{VI})$, $X_{Mg}^{mus} = Mg/(Fe^{2+} + Mg + Al^{VI})$, and $X_{Al}^{mus} = Al^{VI}/(Fe^{2+} + Mg + Al^{VI})$, respectively, in muscovite.

2.3. Regression model

Inserting Eqs. (3) and (7) into Eq. (2) and rearrange it, a temperature-dependent regression model was obtained:

$$\begin{aligned}T = &(\Delta H^0/\Delta S^0) + (P-1)(\Delta V^0/\Delta S^0) \\ &+ (W_{FeMg}^{mus}/\Delta S^0) \cdot 3(X_{Fe}^{mus} - X_{Mg}^{mus}) \\ &+ [(W_{MgAl}^{mus} - W_{FeAl}^{mus})/\Delta S^0] \cdot 3X_{Al}^{mus} \\ &+ (1/\Delta S^0)[3RT\ln K_d + GaT + GbP + Gc]\end{aligned} \quad (8)$$

which is actually a curve equation in a multidimensional space and may be resolved through iterative multiple regression.

3. Natural metapelitic rocks: data set

Empirical calibration of a geothermometer requires natural rock samples with well-determined chemical compositions of coexisting minerals, and pressures and temperatures of equilibration. For this, we collected 73 samples of pelitic metamorphic rocks from the literature. The pressures and temperatures range from 3.0–14.0 kbar to 530–700 °C, respectively.

The samples all fit the following four criteria: (1) there is a clear description of textural equilibria among garnet, biotite, muscovite, plagioclase, quartz, kyanite and/or sillimanite in the literature; (2) there are also detailed electron microprobe analyses of the minerals involved, at least SiO_2, TiO_2, Al_2O_3, FeO, MnO, MgO, CaO, Na_2O and K_2O were analyzed. If there is chemical zoning in garnet, only the rim composition is used, and accordingly, only the (rim) compositions of matrix biotite, muscovite and plagioclase in contact with garnet are used; (3) stoichiometry of the analyzed minerals are confirmed; and (4) the samples did not undergo retrogression. The samples are listed in Table 1.

Equilibrium temperatures and pressures of the natural metapelitic samples (Table 1) collected from the literature were determined by simultaneously applying the garnet–biotite thermometer (Holdaway, 2000) and the GASP barometer (Holdaway, 2001).

At present, there are nearly 30 versions of the garnet–biotite thermometer available, among which only the Holdaway (2000) version yields the smallest absolute error (± 25 °C) in reproducing the experimental temperatures of Ferry and Spear (1978), Perchuk and Lavrent'eva (1983) and Gessmann et al. (1997), in the wide range 550–950 °C. Furthermore, this thermometer may successfully discern the systematic change of temperatures of rocks from different zones of prograde sequences, inverted metamorphic zones, and thermal contact aureoles. Uncertainty of ± 2.0 kbar of input pressure may introduce small errors of ± 3–6 °C of garnet–biotite temperatures for common metapelites. Thus, this thermometer is believed to be a reliable and precise tool.

GASP barometer is valid only for higher anorthite contents in plagioclase and higher grossular contents in garnet (Todd, 1998; Holdaway, 2001). In many metapelites, the mole fraction of grossular in garnet is $<10\%$, and in typical metapelites, the anorthite com-

Table 1
Natural metapelites for calibrating the garnet–muscovite thermometry

Source	Sample	Al-phase	GASP	$T_{(gb)}$	$T_{(A)}$	$T_{(B)}$	Source	Sample	Al-phase	GASP	$T_{(gb)}$	$T_{(A)}$	$T_{(B)}$
T78	892U	Sill	4219	610	598	603	G91	2038	–	3866**	579	574	580
	869	Sill	4120	595	594	599		2040-2.	Sill	3866	600	592	585
	871	Sill	3713	613	591	597	HR84	8B	Ky	9705	708	701	695
	C26A	Sill	2846	593	577	584		8C	Ky	6939	570	602	607
	595C	Sill	5955	695	672	669		12E	Ky	5114	563	592	602
SG89	S129	Ky	5941	623	601	608		18A	Ky	7320	579	566	568
	S130	Ky	6205	631	602	608		21A	Ky	6416	606	651	641
	S134A	Ky	6748	613	601	608		21C	Ky	7709	615	642	644
	S135	Ky	7620	643	616	617		21F	Ky	6657	606	621	628
	S141G	Ky	6266	626	606	610	SB87	SA-19	Ky	7311	575	605	607
	S142A	Ky	7069	654	622	621		SA-5	Ky	7700	594	606	609
H89	CC-33a	Ky	6896	641	611	611		S-306	Ky	8871	620	622	625
	CC-36	Ky	8237	667	610	600	E95	Fus80b	Ky	10,448	592	612	614
H91	23A	And	4169	580	598	601		Ma9353	Ky	5089	648	619	621
	1004A	And	3899	580	616	617		Ma9355	Ky	14,006	636	600	598
	906A	And	4085	586	595	600		Ma9356	Ky	10,447	650	619	620
	1001A	And	4918	594	575	582		Ma9356	Ky	12,331	656	684	689
	24A	Sill	4910	617	622	623		Ma9364	Ky	5535	649	608	613
	905A	Sill	4652	605	602	605		Ma9364	Ky	6066	651	608	612
	663A	Sill	4801	613	617	617		Mag096	Ky	5678	596	585	591
	666A	Sill	4046	597	587	594		Mag310	Sill	6430	640	626	630
WD98	ND9522	Sill*	2963	609	594	597		Mag431	Ky	11,548	695	698	698
Z96	162-2	Ky	11,255	530	543	552		Mag452	Ky	4847	603	580	587
	181-1	Ky	11,702	547	559	560		Mag540	Ky	6532	656	617	620
	181-2	Ky	11,466	544	534	538	TE97	Ma9415	Ky + Sill	5193	592	589	596
ZC99	S4-1M2	Ky	7834	604	580	582		Ma9418	Sill	6548	611	592	596
	S4-2M2	Ky	8179	600	581	584		Ma9421	Sill	5888	634	584	589
	S4-3M2	Ky	7801	584	583	585		Ma9422	Sill	4941	606	594	599
	Z-3M2	Ky	4605	535	582	584		Ma9429	Ky + Sill	7829	652	625	625
	D6-2M2	Ky	6129	605	599	600		Ma9450	Ky	8507	641	639	633
	162-2M2	Ky	12,476	561	561	567		Ma9464	Ky	7058	559	595	604
	181-1M2	Ky	12,502	567	574	573		Ma9506	Ky + Sill	5883	644	620	619
	181-2M2	Ky	12,290	564	548	550		Si9414	Ky	7545	622	619	620
G94	gsg92.9	Ky	4432	597	583	593		T024	Ky + Sill	7879	603	628	626
	c91-14	Ky	5824	635	602	596		T024	Ky + Sill	10,154	609	630	626
G91	1001	–	3866**	556	563	569		T031	Ky	5840	606	606	607
	2025A	–	3866**	556	564	571		T031	Ky	5895	611	609	610

Note: GASP and $T_{(gb)}$ are GASP pressures (Holdaway, 2001) and garnet–biotite temperatures (Holdaway, 2000), respectively. *: Metamorphic granite. **: These samples were collected within 600 m, so pressure was assumed as the same. $T_{(A)}$ and $T_{(B)}$ are the garnet–muscovite temperatures of Models A and B determined in this work, respectively. Sample source abbreviations: T78 = Tracy (1978), SG89 = Sevigny and Ghent (1989), H89 = Hoisch (1989), H91 = Hoisch (1991), WD98 = Whitney and Dilek (1998), Z96 = Zhao et al. (1996), ZC99 = Zhao and Cawood (1999), G94 = Gordon et al. (1994), G91 = Gordon et al. (1991), HR84 = Hodges and Royden (1984), SB87 = Steltenpohl and Bartley (1987), E95 = Engi et al. (1995), TE97 = Todd and Engi (1997). Pressure is in bar and temperature is in °C.

ponent of plagioclase is commonly less than 30% (Todd, 1998). After theoretical modelling and analyses of natural metapelites, Todd (1998) pointed out that GASP barometer should be used with great caution when Xan < 30% and/or Xgros < 10%. After refinement of this barometer, Holdaway (2001) stated that it can be used for Xan > 17% and Xgros>3%. Of the 70 samples used to calibrate the garnet–muscovite thermometer, only 11 samples are slightly anorthite-deficient, but all the garnets of the 70 samples exceed 3% grossular. Thus, these samples are believed to be suitable for calibration.

To satisfy internal thermodynamic consistency with the Holdaway (2000, 2001) thermobarometry,

we assumed that there is 3% ferric iron in garnet, and 11.6% ferric iron in biotite for the natural metapelites (Table 1), as Holdaway (2000, 2001) did in calibrating his thermobarometer.

Ferric iron content in muscovite is still an unresolved problem for petrologists. Miller et al. (1981) analyzed 41 samples of plutonic muscovite through Mössbauer spectra and found that $Fe^{3+}/(Fe^{2+}Fe^{3+})$ in muscovite is as high as 0.8 in magmatic rocks. However, the samples involved in this work are not magmatic but metamorphic. Guidotti et al. (1994) measured a great body of metapelitic muscovites through Mössbauer spectroscopy, and found that the average Fe^{3+}/Fe_{tot} ratio of muscovite is 0.45 ± 0.11 for graphite-bearing samples, and 0.67 ± 0.06 for magnetite-bearing samples.

Due to the problem of determining ferric iron contents, in this work, ferric iron contents of muscovite were assumed to be 0% and 50%, and these two treatments were designated as Models A and B, respectively. We state herein that such treatments are somewhat arbitrary, but these two treatments have almost identical results, because the derived parameters for the two thermometer models are different, as we may see later. On the other hand, zero ferric iron contents of muscovite are always assumed elsewhere in most literature. The Fe_{tot} and Mg atoms of muscovites (Table 1) are in the ranges of 0.03–0.17 and 0.04–0.14, respectively, on the 11-oxygen basis.

The temperatures of the natural samples (Table 1) are not equally distributed, and they generally cluster in the range 550–650 °C. In the computation, some samples were hired for more than two times, such that the samples belonging to 500–550, 551–600, 601–650, and 651–700 °C ranges could be used in the calculation by almost equal quantities.

4. Calibration

Substituting the data listed in Table 1 into Eq. (8) to construct a set of over-determined equations, and using iterative regression computation, we arrived at: (1) for the data set with the assumption of no ferric iron in muscovite (Model A), $\Delta H^0/\Delta S^0 = 969.9$ (± 95.7) K, $\Delta V^0/\Delta S^0 = 1.3$ (± 0.9) K/kbar, $W^{mus}_{FeMg}/\Delta S^0 = -1464.6$ (± 70.7) K, $(W^{mus}_{MgAl} - W^{mus}_{FeAl})/\Delta S^0 = 66.8$ (± 35.0) K, $1/\Delta S^0 = -0.0091$ (± 0.0005) K/J, and a multiple correlation coefficient of $R = 0.91$ was derived from the regression; and (2) for the data set with the assumption of 50% ferric iron in muscovite (Model B), $\Delta H^0/\Delta S^0 = -1167.3$ (± 255.0) K, $\Delta V^0/\Delta S^0 = -0.2$ (± 1.0) K/kbar, $W^{mus}_{FeMg}/\Delta S^0 = -2292.7$ (± 152.0) K, $(W^{mus}_{MgAl} - W^{mus}_{FeAl})/\Delta S^0 = 823.0$ (± 92.7) K, $1/\Delta S^0 = -0.0088$ (± 0.0007) K/J, and a multiple correlation coefficient of $R = 0.90$ was derived. Inserting these parameters into Eq. (8), we have gained two new formulations of the garnet–muscovite Fe–Mg exchange geothermometry:

(a) Model A, assuming no ferric iron in muscovite

$$T_{(A)}\ (\mathrm{K}) = \frac{969.9 + P\ (\mathrm{kbar})\ (1.3 - 9.1\mathrm{Gb}) - 0.0091\mathrm{Gc} - 4393.8(X^{mus}_{Fe} - X^{mus}_{Mg}) + 200.4X^{mus}_{Al}}{1 + 0.0091(3R\ln K_d + \mathrm{Ga})} \quad (9a)$$

and

(b) Model B, assuming 50% Fe^{3+} contents in muscovite

$$T_{(B)}\ (\mathrm{K}) = \frac{-1167.3 - P\ (\mathrm{kbar})\ (0.2 + 8.8\mathrm{Gb}) - 0.0088\mathrm{Gc} - 6878.1(X^{mus}_{Fe} - X^{mus}_{Mg}) + 2469.0X^{mus}_{Al}}{1 + 0.0088(3R\ln K_d + \mathrm{Ga})} \quad (9b)$$

5. Error analysis

The total uncertainty of one thermometer includes systematic and random errors. The best way for evaluating systematic error is to apply the thermometer to experimental data and examine the difference between calculated and experimental temperatures. However, at present, there are no experimental data for metapelites available, so here, we just discuss the random error of the two formulations.

Each of the two formulations (Eq. (9a,b)) is a continuous function of pressure, Fe, Mg, and Al^{VI}

Table 2
Applications of the garnet–muscovite thermometers of this work to the natural metapelites not included in calibrating the thermometry

Source	Sample	Al-phase	P	$T_{(gb)}$	$T_{(A)}$	$T_{(B)}$	Source	Sample	Al-phase	P	$T_{(gb)}$	$T_{(A)}$	$T_{(B)}$
HS84	78B	Sill	5458	557	561	567	WS91	284-2	–	5000*	556	530	537
	80D	Sill	4281	567	571	577	H90	W228	–	5000*	606	585	587
	90A	Sill	5193	570	573	579		CC25c	–	5000*	593	607	610
	92D	Sill	5353	567	566	572	KS93	K87-83J	–	5000*	563	553	561
	145E	Sill	5120	567	555	561		K87-83L	–	5000*	543	511	521
	146B	Sill + And	4374	594	623	623		K87-83N	–	5000*	557	520	527
	146D	Sill + And	3750	564	577	584		K87-20B	– **	5000*	553	530	535
NH81	147	And	5000*	576	585	588		K87-21E	– **	5000*	560	592	604
	AH1	And	5000*	586	592	596		K90-15A	–	5000*	589	581	580
	91	And	5000*	580	584	587		K90-15C	–	5000*	588	551	555
	41	Sill + And	5000*	588	594	598	K93	CD169D2	–	5000*	593	573	579
	5	Sill + And	5000*	570	577	581		CD171D	–	5000*	595	577	581
	102	Sill + And	5000*	572	567	572		SP-9B1	Ky	5000*	591	622	623
	EW3	Sill	5000*	589	593	595		SP-9G4	–	5000*	598	588	593
	MA4	Sill + And	5000*	608	603	607		CD-201E	–	5000*	614	614	615
	107	Sill	5000*	575	587	591		CD201G	–	5000*	613	606	610
P82	373	Ky	5975	595	579	585		VI2C	–	5000*	613	592	598
	121	Ky	5286	589	585	590	B89	260Br	–	5000*	570	602	610
	367	Ky + Sill	6165	603	592	596		268Br	–	5000*	596	617	622
	82	Ky + Sill	5161	581	578	583		836Br	–	5000*	572	603	609
	398	Ky + Sill	4816	585	575	581		R60r	–	5000*	574	567	575
	492	Ky + Sill	4926	585	590	594		R223r	–	5000*	575	618	621
	223	Ky + Sill	4910	585	585	590	B92	191r	–	5000*	568	565	573
	2-376	Ky + Sill	6076	599	592	595		241r	–	5000*	607	638	644
	2-13.	Sill	5319	582	576	580		26r	–	5000*	580	587	593
	74	Sill	5760	614	599	598		137r	–	5000*	631	643	645
	59	Sill	5943	603	590	594		189r	–	5000*	605	556	562
	40	Sill	4791	584	585	590	Z96	S4-1	–	5000*	593	577	582
C87	Irim	And	5000*	548	515	524		S4-2	–	5000*	590	579	584
	IIArim	And	5000*	541	546	549		S4-3	–	5000*	577	581	585
	IIArim	And	5000*	555	546	549		Z3-2	–	5000*	578	584	586
	IIArim	And	5000*	573	546	549		Z-3	–	5000*	581	578	583
	IIBrim	And	5000*	552	548	542		D6-2	–	5000*	607	585	588
	IIBrim	And	5000*	529	533	529	ZC99	N30-4M1	–	5000*	535	583	588
	IIIrim	Sill	5000*	587	579	576		S4-1M1	–	5000*	469	491	504
FG79	5	Ky	8690	540	548	555		S4-3M1	–	5000*	481	483	485
	6	Sill	9869	593	598	599		Z3-2M1	–	5000*	463	480	496
	7	Sill	1422	614	616	622		162-2M1	–	5000*	489	546	555
	8	Sill	8311	609	609	609		181-2M1	–	5000*	501	540	552
	10	Sill	4644	602	602	608	HF88	615r	–	5000*	521	505	518
	12	Sill	5347	608	606	609		621r	–	5000*	522	536	549
	13	Sill	4657	620	621	622		622r	–	5000*	531	524	536
	9	Sill	5390	583	593	598	KA93	BGR2	–	5000*	518	553	559
	11	Sill	4993	622	620	622		BGR6	–	5000*	552	546	554
	14	Sill	6033	628	599	602		BGR17	–	5000*	538	571	584
	15	Sill	8197	628	585	586		BGR19	–	5000*	535	540	552
H88	2	–	5000*	581	595	601		BGR19	–	5000*	608	586	595
	96	–	5000*	552	554	560		BGR73	–	5000*	522	552	562
	1A	–	5000*	585	601	604	SB87	SB42	–	5000*	638	594	600
	52	–	5000*	570	580	584		SA-34	–	5000*	576	561	569
	3A	–	5000*	582	605	607		S-140	–	5000*	563	600	608
	61A	–	5000*	584	599	602		S-100	–	5000*	543	561	570
	84	–	5000*	566	556	562		SA-374	–	5000*	562	590	596

Table 2 (*continued*)

Source	Sample	Al-phase	P	$T_{(gb)}$	$T_{(A)}$	$T_{(B)}$	Source	Sample	Al-phase	P	$T_{(gb)}$	$T_{(A)}$	$T_{(B)}$
	129	–	5000*	607	552	560		SA-349	–	5000*	564	591	598
	114	–	5000*	568	569	574		SA-376	–	5000*	524	575	581
	5A	–	5000*	603	605	607		SB47B	–	5000*	618	605	613
	65	–	5000*	567	554	562	H78	PR-53A	–	5000*	578	556	564
	94	–	5000*	597	590	593		PR-53C	–	5000*	612	572	577
	27	–	5000*	573	554	558		PR-62	–	5000*	597	570	576
WS91	106-3	–	5000*	564	569	573		PR-25A	–	5000*	566	557	566
	107-1	–	5000*	563	547	554		PR-74D	–	5000*	591	580	586
	108-1	–	5000*	553	525	536		PR-78A	–	5000*	594	570	577
	193-1	–	5000*	554	533	541		PR-67C1	And + Sill	5000*	642	705	692
	199-1	–	5000*	560	551	556							

Note: P and $T_{(gb)}$ are GASP pressures (Holdaway, 2001) and garnet–biotite temperatures (Holdaway, 2000), respectively, except for that labeled " * " were assumed pressures. **: amphibolite. Sample source abbreviations: HS84 = Hodges and Spear (1984), NH81 = Novak and Holdaway (1981), P82 = Pigage (1982), C87 = Clarke et al. (1987), FG79 = Fletcher and Greenwood (1979), H88 = Holdaway et al. (1988), WS91 = Wang and Spear (1991), H90 = Hoisch (1990), KS93 = Kohn and Spear (1993), K93 = Kohn et al. (1993), B89 = Burton et al. (1989), B92 = Bergman (1992), Z96 = Zhao et al. (1996), ZC99 = Zhao and Cawood (1999), HF88 = Hynes and Forest (1988), KA93 = Kamber (1993), SB87 = Steltenpohl and Bartley (1987), H78 = Holdaway (1978). Pressure is in bar and temperature is in °C.

components in muscovite, and Fe, Mg, Mn and Ca components in garnet. Thus, neglecting the correlations of the analytical errors of mineral components, total random error of the garnet–muscovite thermometer stem from pressure uncertainty and analytical errors of minerals may be written as

$$\begin{aligned}\Delta T_{\mathrm{gm}} = &\left(\frac{\partial T}{\partial P}\right)\Delta P + \left(\frac{\partial T}{\partial X_{\mathrm{Fe}}^{\mathrm{grt}}}\right)\Delta X_{\mathrm{Fe}}^{\mathrm{grt}} \\ &+ \left(\frac{\partial T}{\partial X_{\mathrm{Mg}}^{\mathrm{grt}}}\right)\Delta X_{\mathrm{Mg}}^{\mathrm{grt}} + \left(\frac{\partial T}{\partial X_{\mathrm{Ca}}^{\mathrm{grt}}}\right)\Delta X_{\mathrm{Ca}}^{\mathrm{grt}} \\ &+ \left(\frac{\partial T}{\partial X_{\mathrm{Mn}}^{\mathrm{grt}}}\right)\Delta X_{\mathrm{Mn}}^{\mathrm{grt}} + \left(\frac{\partial T}{\partial X_{\mathrm{Fe}}^{\mathrm{mus}}}\right)\Delta X_{\mathrm{Fe}}^{\mathrm{mus}} \\ &+ \left(\frac{\partial T}{\partial X_{\mathrm{Mg}}^{\mathrm{mus}}}\right)\Delta X_{\mathrm{Mg}}^{\mathrm{mus}} + \left(\frac{\partial T}{\partial X_{\mathrm{Al}}^{\mathrm{mus}}}\right)\Delta X_{\mathrm{Al}}^{\mathrm{mus}}\end{aligned} \tag{10}$$

in which the delta items stand for the respective errors of the corresponding items. On the basis of Eq. (10) and Tables 1, 2 and 3, we arrived at: (1) pressure estimation has negligible effect on garnet–muscovite temperatures; (2) assuming pressure uncertainty of ±2 kbar and analytical error of ±5% for the relevant compositions of both garnet and muscovite, the total random uncertainty of the thermometer will generally be below ±5 °C. These conclusions are valid for the two formulations of the thermometry.

6. Test and application of the thermometers

The new thermometers (Eq. (9a,b)) have a resolution of ±50 °C in reproducing the input garnet–biotite temperatures (Table 1; Fig. 1). Samples not included in calibrating the thermometers, listed in Tables 2 and 3, may be used to certify their applicability. From Tables 2 and 3 and Fig. 2, we may see that the differences of the garnet–muscovite and garnet–biotite temperatures are well within 50 °C. Furthermore, the two garnet–muscovite thermometers have much more steep dP/dT slopes than the garnet–biotite thermometer (Holdaway, 2000), which imply that they are much more independent of pressure estimate (Fig. 3).

The two garnet–muscovite thermometers, assuming either no ferric iron or 50% ferric iron in muscovite, respectively, gave generally identical temperatures (Fig. 4).

The difference between garnet–biotite and garnet–muscovite temperatures is equally distributed in the range of Xcel = 6–28% (Fig. 5a,b).

Practical thermometers should discriminate different grade rocks from different zones in either prograde

Table 3
Applications of the two new garnet–muscovite thermometers to the metapelites of the prograde, inverted and contact aureole zones

Source	Sample	Al-phase	Zone	P	$T_{(gb)}$	$T_{(A)}$	$T_{(B)}$
LR85	TS29	–	chl-bio	6000*	526	510	519
	BT144	–	grt	6000*	545	546	552
	TS2	–	grt	6000*	526	533	540
	BT91	–	grt	6000*	557	565	572
	BT86	–	stau	6000*	554	550	557
	BT174	–	stau	6000*	566	576	581
	BT137	–	stau	6000*	572	601	605
	BT41	Ky	transition	6692	580	588	591
	BT28	Ky	transition	6581	581	599	603
	BT49	Ky	stau-ky	6714	584	594	596
	BT34	Ky	stau-ky	5627	568	577	583
	BT32	Ky	stau-ky	6206	595	607	610
	BT31	Ky	ky	7720	605	629	628
H91	15A	–	grt	8000*	582	566	569
	20B	–	grt	8000*	597	608	603
	21A	–	stau-bio	8000*	600	630	631
	84B	–	stau-bio	8000*	602	620	621
	88D	Ky	lower ky-bio	11107	637	640	629
	89B	Ky	lower ky-bio	9429	635	613	611
	81C	Ky	higher ky-bio	7872	673	645	642
	83A	Ky	higher ky-bio	8701	655	633	636
	51A	Sill	sill	6329	670	659	653
VG98	48	Ky + Sill	migmatite	5665	614	598	600
	49	Ky + Sill	migmatite	5170	600	564	571
	50	Ky + Sill	migmatite	5596	601	568	572
	52	–	migmatite	5000*	538	497	509
	54	Ky + Sill	migmatite	5045	608	593	597
	55	Ky + Sill	migmatite	5317	605	595	599
	56	Sill	migmatite	4146	583	581	586
	57	Ky + Sill	migmatite	4253	576	595	598
	59	Ky + Sill	sill	5140	599	599	599
	60	Ky + Sill	ky	5128	583	584	591
	62	Ky	ky	5888	593	592	595
	63	–	stau	5000*	583	539	547
	65	–	stau	5000*	569	567	571
	66	–	stau	5000*	600	551	557
	73	–	stau	5000*	548	545	554
D84	17	–	bio	7000*			
	86	–	grt	7000*	540	543	550
	55	–	stau	7000*	617	623	619
	154	Ky	ky	6995	650	626	625
	153	Ky	ky	6771	647		

Note: P and $T_{(gb)}$ are GASP pressures (Holdaway, 2001) and garnet–biotite temperatures (Holdaway, 2000), respectively, except for that labeled " * " were assumed pressures. Sample source abbreviations: LR85 = Lang and Rice (1985), H91 = Himmelberg et al. (1991), VG98 = Vannay and Grasemann (1998), D84 = Delor et al. (1984). Pressure is in bar and temperature is in °C.

sequences, or inverted metamorphic zones, or thermal contact aureoles. We check the usefulness of our garnet–muscovite thermometry hereafter.

6.1. Prograde sequence

Lang and Rice (1985) described a prograde sequence of metapelites, that is, the consequence of the second period of regional metamorphism in the Snow Peak area, northern Idaho, USA. Considering that the Prichard Formation (from which TS29 was sampled) was emplaced on top of the upper Wallace Formation

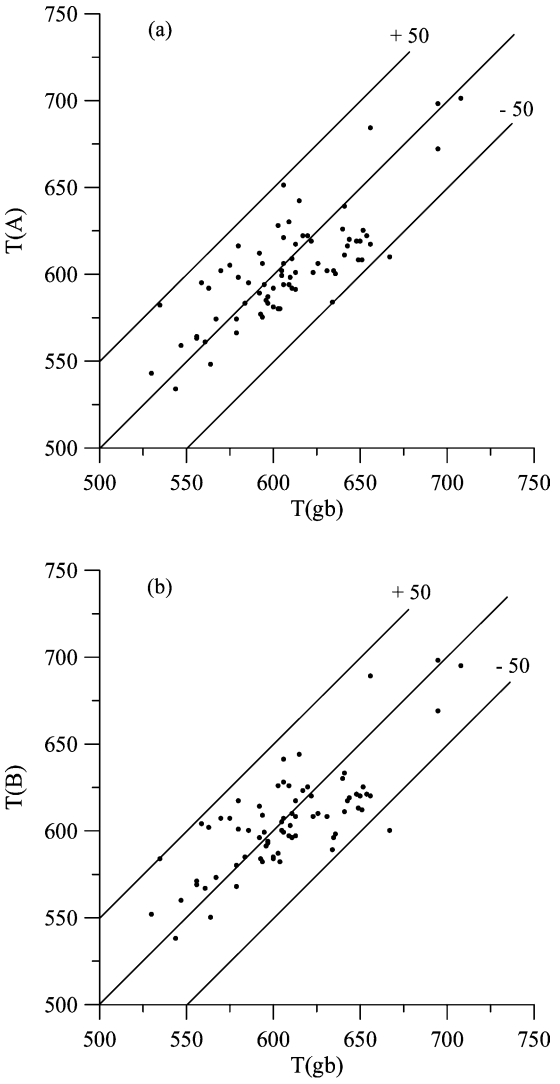

Fig. 1. Garnet–muscovite vs. garnet–biotite temperatures. (a) Garnet–muscovite thermometer (Model A); (b) garnet–muscovite thermometer (Model B). Dots stand for samples in Table 1, which were included in calibrating the garnet–muscovite thermometry. Temperature is in °C.

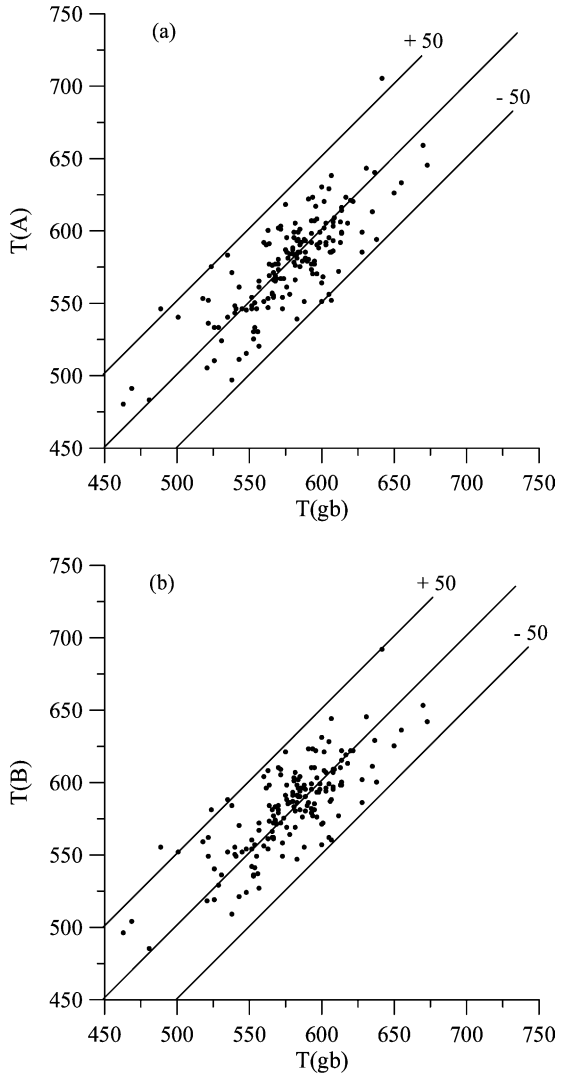

Fig. 2. Garnet–muscovite vs. garnet–biotite temperatures. (a) Garnet–muscovite thermometer (Model A); (b) garnet–muscovite thermometer (Model B). Dots stand for samples in Tables 2 and 3, which were not included in calibrating the garnet–muscovite thermometry. Temperature is in °C.

(from which TS2 was sampled) before regional metamorphism, and the close geographic proximity of the samples, the pressure of equilibration of the

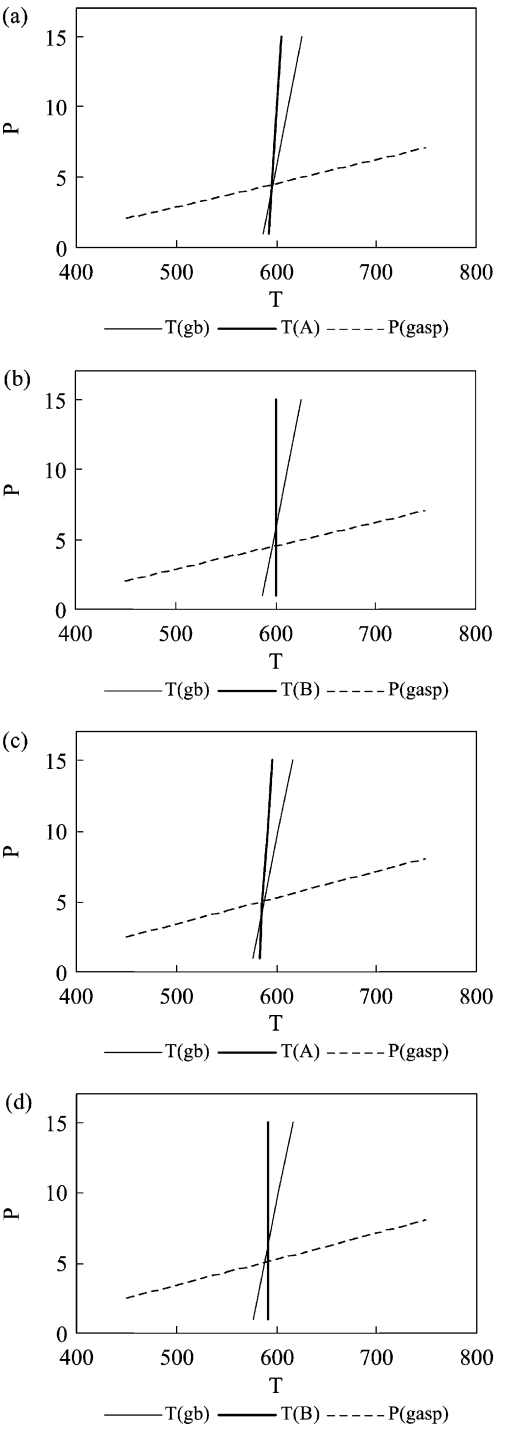

Fig. 3. *P*/*T* slops of garnet–muscovite vs. garnet–biotite thermometers. (a) Sample 905A, Model A; (b) sample 905A, Model B; (c) sample 121, Model A; (d) sample 121, Model B. Sample 905A was included, while sample 121 was not included, in calibrating the thermometry. Pressure is in kbar and temperature is in °C.

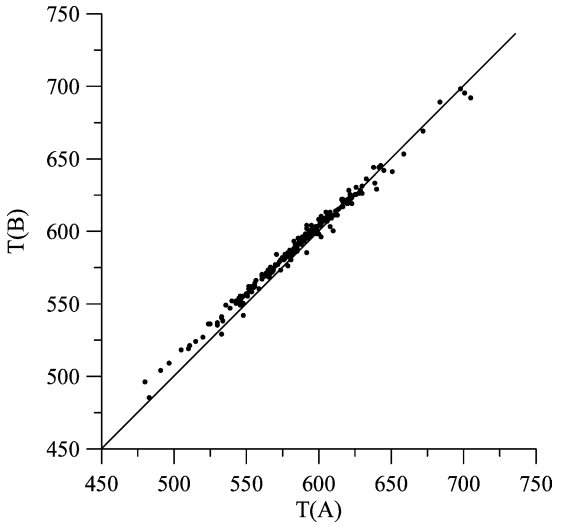

Fig. 4. Comparison of temperatures of Model A vs. Model B. Dots stand for samples in Tables 1, 2 and 3. Temperature is in °C.

chlorite–biotite and garnet zones was reasonably assumed to be 6 kbar. This is similar to the pressures obtained from GASP barometer (Holdaway, 2001) for the nearby sillimanite- and/or kyanite-bearing rocks. The resulting garnet–biotite temperatures are: for the chlorite–biotite zone, 526 °C; for the garnet zone, 526–557 °C; for the staurolite zone, 554–572 °C; for the transition zone, 580–581 °C; for the staurolite–kyanite zone, 568–595 °C; and for the kyanite zone, 605 °C (Table 3). Here, the garnet–biotite thermometer (Holdaway, 2000) successfully distinguished the different grade rocks. Our two garnet–muscovite thermometers yielded identical results and all gave temperatures very close to the garnet–biotite temperatures (Table 3). The temperature difference for the prograde zones is obvious: (1) Model A gave 510, 533–565, 550–601, 588–589, 577–607 and 629 °C, respectively; and (2) Model B gave 519, 540–572, 557–605, 591–603, 583–610 and 628 °C, respectively.

6.2. Inverted metamorphic zones

An inverted metamorphic gradient is preserved in the western metamorphic belt near Juneau, AK. Himmelberg et al. (1991) stated that the western metamorphic belt is part of the Coastal plutonic–metamorphic complex of western Canada and southeastern Alaska that developed as a result of tectonic overlap and/or compressional thickening of crustal rocks during collision of the Alexander and Stikine terranes. Detailed mapping of pelitic single-mineral isograds, systematic changes in mineral assemblages, and silicate geothermometry indicate that thermal peak metamorphic

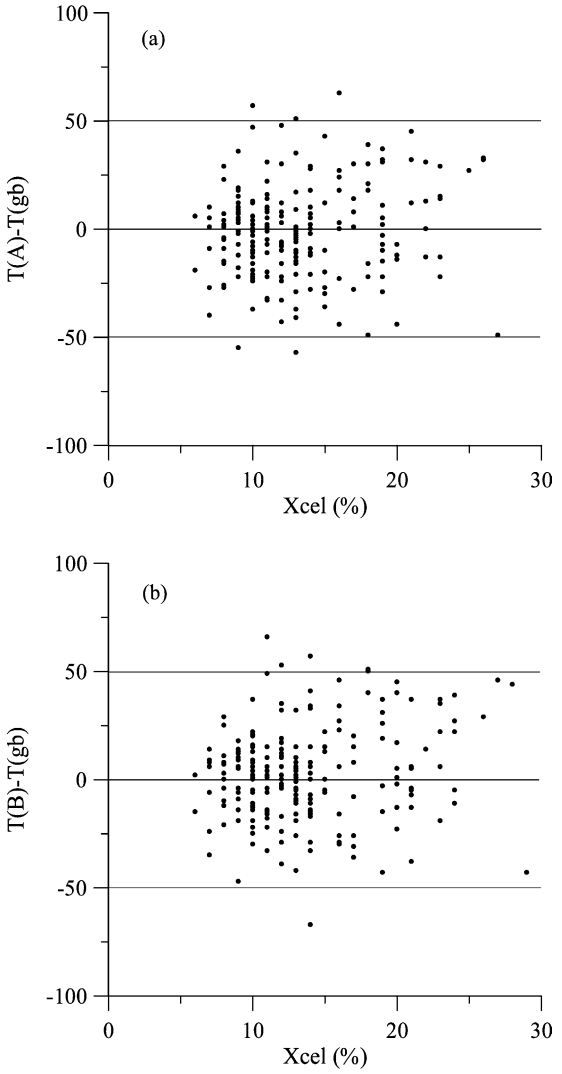

Fig. 5. Celadonite fraction in muscovite vs. the difference between garnet–muscovite and garnet–biotite temperatures. Dots stand for samples in Tables 1, 2 and 3. (a) Model A; (b) Model B. Celadonite fraction is defined as $X_{cel}=4X_{Mg}^{mus}X_{Al}^{mus}$ (mixing-on-sites model). Temperature is in °C.

conditions increase structurally upward over a distance of about 8 km. From bottom to top, there gradually outcrops rocks of green biotite, brown biotite, garnet, staurolite–biotite, lower kyanite–biotite, upper kyanite–biotite and sillimanite zones. Garnet–biotite thermometer (Holdaway, 2000) successfully discriminated the different zone rocks, and again, our two garnet–muscovite thermometers gave similar results, and distinguished the different zone rocks (Table 3). However, Model B yielded higher temperatures for the staurolite zone rocks than the lower kyanite–biotite ones, which is not the case.

The crystalline core of the Himalayan orogen in the Sutlej valley corresponds to a 9-km-thick, high-grade metamorphic sequence. This High Himalayan Crystalline (HHC) shows an inverted metamorphic zonation characterized, from the base to the top of the unit, by a gradual superposition of staurolite, kyanite, sillimanite, and migmatite Barrovian mineral zones (Vannay and Grasemann, 1998). Garnet–biotite thermometer (Holdaway, 2000) confirmed the gradual increase of temperature from the bottom to the top of the sequence, our two garnet–muscovite thermometers also clearly reflected such a trend, and they gave identical temperatures (Table 3).

6.3. Thermal contact aureole

In Eastern Rouergue, France, garnet, staurolite and kyanite isograds in metasedimentary rocks were developed as a result of thermal metamorphism around syntectonic granitoids, and the biotite, garnet, staurolite and kyanite zones were mapped (Delor et al., 1984). For the kyanite zone, samples 154 and 153, simultaneously applying the garnet–biotite thermometer (Holdaway, 2000) and the GASP barometer (Holdaway, 2001), yielded pressures of 6.77–7.0 kbar and temperatures of 647–650 °C. For other samples devoid of kyanite and/or sillimanite, we assumed a pressure of 7.0 kbar. This yielded garnet–biotite temperatures of 540 and 617 °C for the garnet and staurolite zones, respectively. Our two garnet–muscovite thermometers gave almost the same results as the garnet–biotite geothermometer and naturally reflected systematic change of the temperature of different zone rocks. Again, the two garnet–muscovite thermometers gave identical temperatures (Table 3).

7. Conclusions

The two garnet–muscovite thermometers, assuming either no ferric iron (Model A) or 50% ferric iron (Model B) in muscovite, respectively, gave generally identical temperatures (Fig. 4), and can be safely used on metapelites in the range 480–700 °C and 3.0–14.0 kbar. The thermometers can distinguish the systematic change of temperature of metapelites from different zones in prograde sequence, inverted metamorphic zone, and thermal contact aureole, thus, they may be applied to natural metapelitic rocks as practical tools.

Acknowledgements

We sincerely thank Prof. M.J. Holdaway for generously sending us his garnet–biotite thermometer and GASP barometer programs. Detailed reviews by C.S. Todd and an anonymous reviewer greatly improved the quality of the original manuscript. This work was jointly supported by the National Natural Science Foundation of China (Grant Nos. 40002017, 40102017, 40072060 and 49872063), a China Geological Survey Project (J2.1.4.), and the National and CAS Tibet Research Project (KZ951-A1-204-01-05, KZ95T-06).

References

Bergman, S., 1992. P–T paths in the Handol area, central Scandinavia: record of Caledonian accretion of outbroad rocks to the Baltoscandian margin. J. Metamorph. Geol. 10, 265–281.

Burton, K.W., Boyle, A.P., Kirk, W.L., Mason, R., 1989. Pressure, temperature and structural evolution of the Sulitjelma foldnappe, central Scandinavian Caledonides. In: Daly, J.S., Cliff, R.A., Yardley, B.W.D. (Eds.), Evolution of Metamorphic Belts. Geological Society Special Publication, vol. 43, pp. 391–411.

Clarke, G.L., Guiraud, M., Powell, R., Gurg, J.P., 1987. Metamorphism in the Olary Block, South Australia: compression with cooling in a Proterozoic fold belt. J. Metamorph. Geol. 5, 291–306.

Delor, C.P., Burg, J.P., Leyreloup, A.F., 1984. Staurolite producing reactions and geothermobarometry of a high pressure thermal aureole in the French Massif Central. J. Metamorph. Geol. 2, 55–72.

Engi, M., Todd, C.S., Schmatz, D.R., 1995. Tertiary metamorphic conditions in the eastern Lepontine Alps. Schweiz. Mineral. Petrogr. Mitt. 75, 347–369.

Ferry, J.M., Spear, F.S., 1978. Experimental calibration of the partitioning of Fe and Mg between biotite and garnet. Contrib. Mineral. Petrol. 66, 113–117.

Fletcher, C.J.N., Greenwood, H.J., 1979. Metamorphism and structure of Penfold Creek area, near Quesnel Lake, British Columbia. J. Petrol. 20, 743–794.

Ganguly, J., Cheng, W., 1994. Thermodynamics of (Ca, Mg, Fe, Mn)-garnet solid solution: New experiments, optimized data set, and applications to thermo-barometry. Int. Mineral. Assoc. 16th General Meeting abstracts, Pisa, Italy, pp. 134–135.

Gessmann, C.K., Spiering, B., Raith, M., 1997. Experimental study of the Fe–Mg exchange between garnet and biotite: constraints on the mixing behavior and analysis of the cation-exchange mechanisms. Am. Mineral. 82, 1225–1240.

Gordon, T.M., Ghent, E.D., Stout, M.Z., 1991. Algebraic analysis of the biotite–sillimanite isograde in the File Lake area, Manitoba. Can. Mineral. 29, 673–686.

Gordon, T.M., Aranovich, L.Ya., Fed'kin, V.V., 1994. Exploratory data analysis in thermobarometry: an example from the Kisseynew sedimentary gneiss belt, Manitoba, Canada. Am. Mineral. 79, 973–982.

Green, T.H., Hellman, P.L., 1982. Fe–Mg partitioning between coexisting garnet and phengite at high pressure, and comments on a garnet–phengite geothermometer. Lithos 15, 253–266.

Guidotti, C.V., Yates, M.G., Dyar, M.D., Taylor, M.E., 1994. Petrologic implications of the Fe^{3+} content in pelitic schists. Am. Mineral. 79, 793–795.

Himmelberg, G.R., Brew, D.A., Ford, A.B., 1991. Development of inverted metamorphic isograds in the western metamorphic belt, Juneau, Alaska. J. Metamorph. Geol. 9, 165–180.

Hodges, K.V., Royden, L., 1984. Geologic thermobarometry of retrograde metamorphic rocks: an introduction of the uplift trajectory of a portion of the northern Scandinavian Caledonides. J. Geol. Res. 89, 7077–7090.

Hodges, K.V., Spear, F.S., 1984. Geothermometry, geobarometry and the Al_2SiO_5 triple point at Moosilauke, New Hampshire. Am. Mineral. 67, 1118–1134.

Hoisch, T.D., 1989. A muscovite–biotite geothermometer. Am. Mineral. 74, 565–572.

Hoisch, T.D., 1990. Empirical calibration of six geobarometers for the mineral assemblage quartz + muscovite + biotite + plagioclase + garnet. Contrib. Mineral. Petrol. 104, 225–234.

Hoisch, T.D., 1991. Equilibria within the mineral assemblage quartz + muscovite + biotite + garnet + plagioclase, and implications for the mixing properties of octahedrally-coordinated cations in muscovite and biotite. Contrib. Mineral. Petrol. 108, 43–54.

Holdaway, M.J., 1978. Significance of chloritiod-bearing and staurolite-bearing rocks in the Picuris Range, New Mexico. Geol. Soc. Am. Bull. 89, 1404–1410.

Holdaway, M.J., 2000. Application of new experimental and garnet Margules data to the garnet–biotite geothermometer. Am. Mineral. 85, 881–892.

Holdaway, M.J., 2001. Recalibration of the GASP geobarometer in light of recent garnet and plagioclase activity models and versions of the garnet–biotite geothermometer. Am. Mineral. 86, 1117–1129.

Holdaway, M.J., Dutrow, B.L., Hinton, R.W., 1988. Devonian and carboniferous metamorphism in west–central Maine: the muscovite–almandine geobarometer and the staurolite problem revised. Am. Mineral. 73, 20–47.

Hynes, A., Forest, R.C., 1988. Empirical garnet–muscovite geothermometry in low-grade metapelites, Selwyn Range (Canadian Rockies). J. Metamorph. Geol. 6, 297–309.

Kamber, B.S., 1993. Regional metamorphism and uplift along the southern margin of the Gotthard massif; results from the Nufenenpass area. Schweiz. Mineral. Petrogr. Mitt. 73, 241–257.

Kohn, M.J., Spear, F.S., 1993. Phase equilibria of margarite-bearing schists and chloritoid + hornblende rocks from western New Hampshire, USA. J. Petrol. 34, 631–651.

Kohn, M.J., Spear, F.S., Dalziel, I.W.D., 1993. Metamorphic P–T paths from Cordillera Darwin, a core complex in Tierra del Fuego, Chile. J. Petrol. 34, 519–542.

Krogh, J.E., Raheim, A., 1978. Temperature and pressure dependence of Fe–Mg partitioning between garnet and phengite, with particular reference to eclogites. Contrib. Mineral. Petrol. 66, 75–80.

Lang, H.M., Rice, J.M., 1985. Regression modelling of metamorphic reactions in metapelites, Snow Peak, Northern Idaho. J. Petrol. 26, 857–887.

Miller, C.F., Stoddard, L.J., Dollase, W.A., 1981. Composition of plutonic muscovite: genetic implications. Can. Mineral. 19, 25–34.

Mukhopadhyay, B., Basu, S., Holdaway, M.J., 1993. A discussion for multicomponent solutions with a generalized approach. Geochim. Cosmochim. Acta 57, 277–283.

Mukhopadhyay, B., Holdaway, M.J., Koziol, A.M., 1997. A statistical model of thermodynamic mixing properties of Ca–Mg–Fe^{2+} garnets. Am. Mineral. 82, 165–181.

Novak, J.M., Holdaway, M.J., 1981. Metamorphic petrology, mineral equilibria, and polymetamorphism in the Augusta quadrangle, south–central Maine. Am. Mineral. 66, 51–69.

Perchuk, L.L., Lavrent'eva, L.Y., 1983. Experimental investigation of exchange equilibria in the system cordierite–garnet–biotite. In: Saxena, S.K. (Ed.), Kinetics and Equilibrium in Mineral Reactions. Advances in Physical Geochemistry, vol. 3. Springer, New York, pp. 199–239.

Pigage, L.C., 1982. Linear regression analysis of sillimanite-forming reactions at Azure Lake, British Columbia. Can. Mineral. 20, 349–378.

Pownceby, M.I., Wall, V.J., O'Neill, H.St.C., 1991. An experimental study of the effect of Ca upon garnet–ilmenite Fe–Mg exchange equilibria. Am. Mineral. 76, 1580–1588.

Sevigny, J.H., Ghent, E.D., 1989. Pressure, temperature and fluid composition during amphibolite facies metamorphism of graphitic metapelites, Haward Ridge, British Columbia. J. Metamorph. Geol. 7, 497–505.

Steltenpohl, M.G., Bartley, J.M., 1987. Thermobarometric profile through the Caledonian nappe stack of western Ofoten, north Norway. Contrib. Mineral. Petrol. 96, 93–103.

Todd, C.S., 1998. Limits on the precision of geobarometry at low grossular and anorthite content. Am. Mineral. 83, 1161–1167.

Todd, C.S., Engi, M., 1997. Metamorphic field gradients in the Central Alps. J. Metamorph. Geol. 15, 513–530.

Tracy, R.J., 1978. High grade metamorphic reactions and partial melting in pelitic schist, west–central Massachusetts. Am. J. Sci. 278, 150–178.

Vannay, J.-C., Grasemann, B., 1998. Inverted metamorphism in the High Himalaya of Himachal Pradesh (NW India): phase equilibria versus thermometry. Schweiz. Mineral. Petrogr. Mitt. 78, 107–132.

Wang, P., Spear, F.S., 1991. A field and theoretical analysis of garnet + chlorite + chloritoid + biotite assemblages from the tri-state (MA, CT, NY) area, USA. Contrib. Mineral. Petrol. 106, 217–235.

Whitney, D.L., Dilek, Y., 1998. Metamorphism during Alpine crustal thickening and extension in central Anatolia, Turkey: the Nigde Metamorphic Core Complex. J. Petrol. 39, 1385–1406.

Zhao, G.C., Cawood, P.A., 1999. Tectonothermal evolution of the Mayuan assemblage in the Cathaysia Block: implications for Neoproterozoic collision-related assembly of the South China Craton. Am. J. Sci. 299, 309–339.

Zhao, G.C., Sun, D.Y., He, T.X., 1996. Buffering of metamorphic reaction temperature by metamorphic fluids in Mayaun Group, Northern Fujian Province. Acta Petrol. Sin. 12, 59–69 (in Chinese with English abstract).